J Mater Sci (2010) 45:34–38
DOI 10.1007/s10853-009-3866-0

A novel chemical reduction route toward fabrication of Fe_3O_4 octahedrons and Fe tubes

DongEn Zhang · Wei Wu · ShanZhong Li · XiaoBo Zhang · GuiQuan Han · Ailing Ying · JunYan Gong · ZhiWei Tong

Received: 17 June 2009 / Accepted: 1 September 2009 / Published online: 8 October 2009
© Springer Science+Business Media, LLC 2009

Abstract Novel Fe_3O_4 octahedrons and Fe microtubes were successfully prepared in different alkaline concentration solutions by the reduction of hematite (α-Fe_2O_3) with hydrazine hydrate. The as-prepared powders were characterized in detail by conventional techniques such as X-ray diffraction and field emission scanning electron microscopy. The role of alkaline concentration during the reaction process is discussed in detail. Compared to the reaction in a water system, the reaction in ethanol required less sodium hydroxide and smaller particles were obtained. In addition, the magnetic properties of the samples were characterized using a vibrating sample magnetometer.

Introduction

Magnetic crystals (magnetite, ferrite, iron, cobalt, nickel, etc.) are widely applied in the fields of information storage, color imaging, bioprocessing, magnetic refrigeration, gas sensing, ferrofluids, etc. [1–4]. Numerous methods have been successfully employed to fabricate magnetic crystals and they can be classified into two categories. One is a thermal or sonochemical decomposition of metal-containing complexes [5–7]. The other is chemical reduction which may comprise hydrogen arc plasma [8], the rapid expansion of supercritical fluid solutions (RESS) in the presence of $LiB(C_2H_5)_3H$ [9], a reduction of ferrous ion association colloids with $NaBH_4$ [10, 11], reduction of hydroxide precursors with hydrogen [12, 13], etc. Among these techniques, chemical reduction is most widely used because of its speed and convenience. However, like the preparation of iron nanocrystals in this method, it remains a challenge because iron salts readily hydrolyze and transform into stable hydroxides which are very difficult to reduce [14]. Boride hydrate is often selected to reduce iron salts in solution but it introduces boride impurities into the product [11]. Among the reductants, hydrazine hydrate has received much attention because of its strong reducing ability, low cost, environmental friendliness, and above all it does not introduce impurities into the system [15]. A variety of metals have been prepared by the reduction of metallic salts with hydrazine hydrate such as copper, silver, ruthenium, nickel, cobalt, iron etc. [16–22].

In this paper, we present a facile method to prepare magnetite octahedrons and iron tubes by reducing hematite (α-Fe_2O_3) with hydrazine hydrate in different alkaline media which helps to avoid the use of toxic materials and complex procedures. Hematite has a rhombohedrally centered hexagonal structure of the corundum type with a close-packed oxygen lattice in which two-thirds of the octahedral sites are occupied by Fe^{3+} ions. Magnetite (Fe_3O_4) crystallizes with a spinel structure. The large oxygen ions are close packed in a cubic arrangement and the smaller iron ions fill in the gaps. The gaps are either a tetrahedral type where iron ion is surrounded by four oxygens or an octahedral type where iron ion is surrounded by six oxygens. The structural formula for magnetite is $[Fe^{3+}]A[Fe^{3+}, Fe^{2+}]BO_4$. This particular

D. Zhang (✉) · S. Li · X. Zhang · G. Han · A. Ying · J. Gong · Z. Tong
Department of Chemical Engineering, HuaiHai Institute of Technology, 222005 Lianyungang, People's Republic of China
e-mail: zdewxm@yahoo.com.cn

W. Wu
Department of Electronics Engineering, Southeast University, 210018 Nanjing, People's Republic of China

D. Zhang · Z. Tong
SORST, Japan Science and Technology Agency (JST), Machida, Tokyo, Japan

arrangement of cations on the A and B sublattice is called an inverse spinel structure. With negative AB exchange interactions the net magnetic moment of magnetite is due to the B-site's Fe^{2+}. Furthermore, the role of the alkaline concentration during the reaction process is discussed in this paper. The products were found to have different qualities that depend on the ethanol and water solvent mixture.

Experimental section

The chemical reagents used in this work were hematite (Fe_2O_3), hydrazine hydrate ($N_2H_4 \cdot H_2O$), and sodium hydroxide (NaOH). All the analytical chemicals were purchased from Shanghai Chemical Reagents Company and used without further purification. A typical synthesis proceeded as follows: an aqueous solution was prepared by dissolving 10 mL hydrazine hydrate ($N_2H_4 \cdot H_2O$), 0.1 g hematite (Fe_2O_3), and different amounts of sodium hydroxide (NaOH) in 30 mL distilled water. After vigorous stirring with a magnetic stirrer bar at room temperature for 10 min, the solution was transferred to a Teflon-lined stainless steel autoclave with a 50 mL capacity. The autoclave was sealed and the solution was kept at 160 °C for 24 h. Upon completion of the reaction, the autoclave was allowed to cool to room temperature. The resultant black solid precipitates were then easily separated from the reaction system by a permanent magnet. The supernatant was discarded by decantation. Distilled water and alcohol were used to wash the precipitates, and this was done several times. Finally, the black products were dried at 80 °C in a vacuum oven.

Characterization

The as-synthesized samples were characterized by X-ray diffraction (XRD, Philips X'Pert PRO SUPER X-ray diffractometer with Cu Kα radiation ($\lambda = 0.154178$ nm), field emission scanning electron microscopy (FE-SEM, JEOL JSM-6700M), and with a vibrating sample magnetometer (VSM, BHV-55).

Results and discussion

It is well known that hydrazine hydrate has a strong reducing ability:

$$N_2 + 4H_2O + 4e^- = N_2H_4 + 4OH^-,\ \Phi^0 = -1.15\,V$$

Therefore, the amount of alkali is a key factor that influences the reaction process. The products obtained by using different amounts of alkali during the reaction process were analyzed by XRD. Without using any alkali the only product was the starting reagent Fe_2O_3 (Fig. 1a) which indicates that no reaction took place. Figure 1b shows that the product obtained in the solution containing 1 g of alkaline was Fe_3O_4. With 10 g of alkali, the characteristic peaks of α-Fe appeared and the product was a mixture of α-Fe and Fe_3O_4 (Fig. 1c). Using 20 g of alkali, a pure α-Fe phase formed (Fig. 1d). At a high alkali concentration the reducing ability of hydrazine was greatly enhanced. Consequently, the reaction between hydrazine and Fe(III) proceeded far more easily. The fact that iron was obtained at a comparatively high alkali concentration further suggests that the alkali concentration is important for the formation of iron.

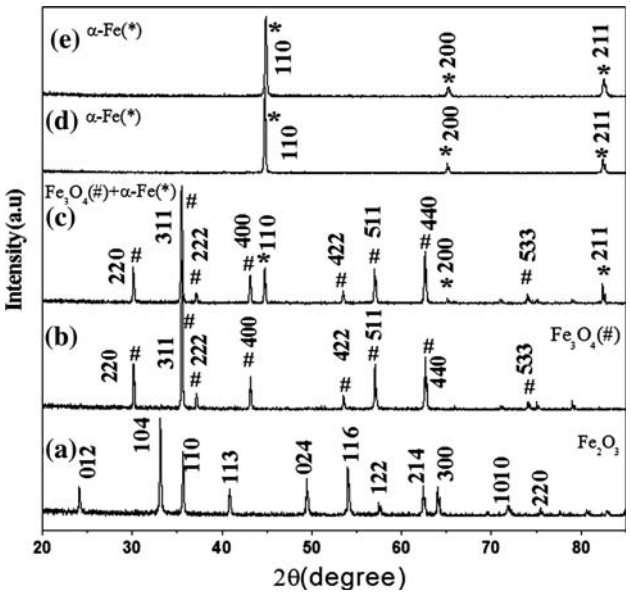

Fig. 1 XRD patterns of the samples produced using different amounts of alkaline: a, b, c, d: in the water system; e: in the ethanol system (*a*) 0; (*b*) 1 g; (*c*) 10 g; (*d*) 20 g; (*e*) 5 g

When water was replaced by ethanol as solvent and with a constant amount of hematite the formation of iron was easier and required less alkali. Figure 1e gives the XRD pattern of the sample produced with 5.0 g sodium hydroxide and this pattern is assigned to a pure α-Fe phase. This phenomenon was also observed in the work of Zheng et al. [23, 24] where they prepared nickel and cobalt nanocrystals using a similar method. This behavior was attributed to the effect of the solvent as it caused the reaction to be more moderate. In water, the precursor of $Fe(OH)_3$ stabilizes easily and is then difficult to reduce [14]. In the case of ethanol, the activity of $Fe(OH)_3$ was almost constant in the presence of ethanol which resulted in milder reaction conditions.

Sizes and morphologies of the Fe_3O_4 samples were studied using FESEM. Figure 2 shows representative FESEM images of the sample prepared in solution with 1 g of alkaline. The low-magnification image in Fig. 2a shows that the magnetite product is composed of octahedrons with

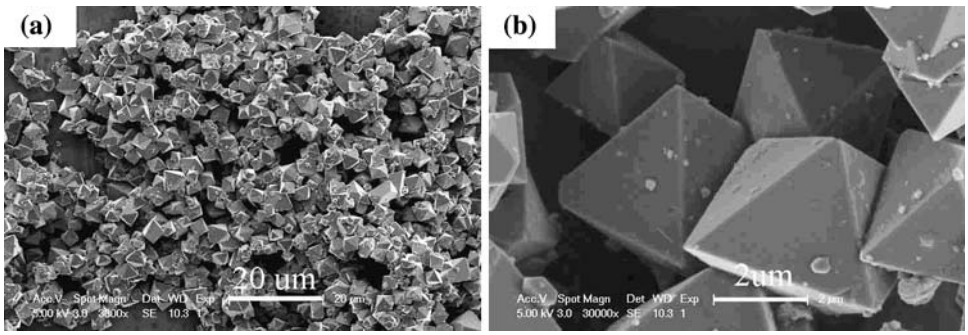

Fig. 2 FESEM images of Fe_3O_4 octahedrons prepared in solution with 1 g of alkaline: **a** low magnification, **b** high magnification

sizes ranging from 2 to 5 μm. These particles display a narrow size distribution as shown in the FESEM image. A high-magnification FESEM image of the magnetite micro-octahedrons is shown in Fig. 2b. These magnetite octahedrons have sharp edges and smooth facets which further indicate that the particles are well crystalline and this is in agreement with the XRD pattern. The morphology of a crystal is mostly determined by the relative growth rate between different planes during its formation. Wang suggested that the morphology of an fcc crystal is determined by the ratio of the growth rate in the ⟨100⟩ direction to that in the ⟨111⟩ direction [25]. Octahedrons bounded by eight {111} planes will be formed when the growth rate along the ⟨100⟩ direction is faster than that along the ⟨111⟩ direction. In our system, the concentration of Fe^{3+} ions was very low in solution because the solubility of Fe_2O_3 particles is very low. Figure 3 shows FESEM images of Fe_2O_3 at different stages during the reaction. Figure 3a shows that the Fe_2O_3 product mainly consists of plates of about 1 μm in size at the start of the reaction. At a reaction time of 3 h, the Fe_2O_3 mainly consisted of nanoparticles that were 200–300 nm in size as shown in Fig. 3b. This figure indicates that Fe_2O_3 was slowly dissolved during the reaction. Therefore, a lower concentration of raw materials leads to a slower reaction rate. In addition, the reaction rate of Fe^{3+} ion reduction to Fe^{2+} ion was slow which contributed to the low formation rate of Fe_3O_4. The slow formation rate is advantageous for a faster growth rate along ⟨100⟩ compared to that along ⟨111⟩. Theoretically, however, the magnetite crystal grows as an octahedron because {111} surfaces have the lowest energy. Slow reaction and growth rates cause magnetite to grow in its typical crystalline habit [26]. At reaction times of 72 h or more the morphology of the Fe_3O_4 samples remained octahedron-like. This indicates that the end shape represents the equilibrium crystal shape.

Figure 4 shows FESEM images of the two Fe samples that were obtained in water and ethanol, respectively. Particles obtained from both the water and ethanol systems were of the same hollow rod shape. However, the particles from the water system (Fig. 4a, b) had sizes ranging from 100 to 120 μm while the particles from the ethanol system (Fig. 4c, d) had sizes ranging from about 10 to 50 μm. It is well known that small metal particles dissolve easily in hot alkali solutions. Therefore, we deduce that an eroding effect of alkali on iron crystals is present. In the water system, the small iron particles dissolved easily because of the higher alkali concentration. In the presence of excess reductant, dissolved particles in the water system could be reduced again. Because of Ostwald ripening, newly produced iron atoms transfer onto the surfaces of larger crystals that have high surface free energies [27–29]. As a result, the final product was relatively larger in size. In ES, however, the eroding effect was much weaker because of the decreased alkali concentration and this contributed to the smaller particle size.

Magnetic measurements on the as-prepared octahedral magnetite were conducted and the M-H hysteresis loop is

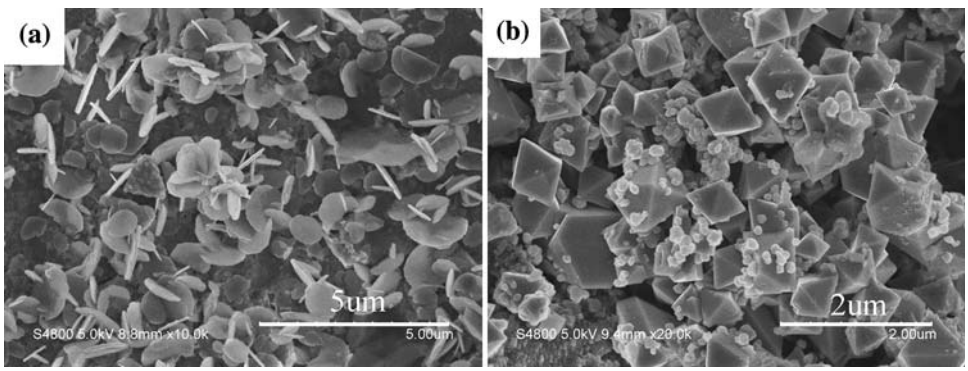

Fig. 3 SEM images of the reaction system with 1 g of alkaline at different times: **a** 0 h, **b** 3 h

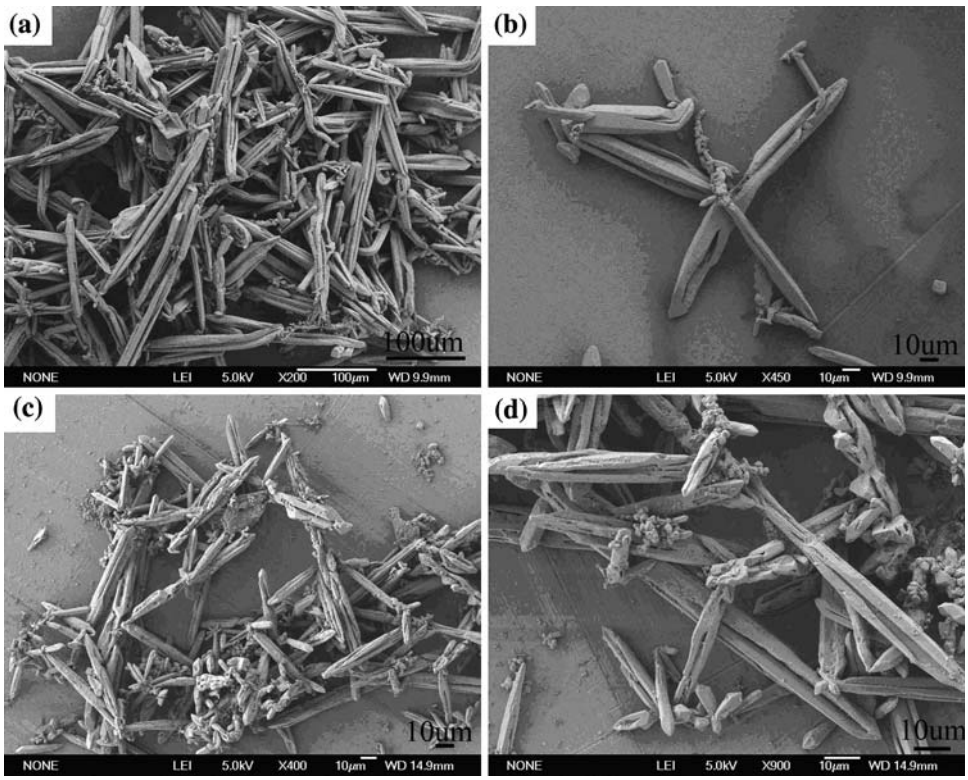

Fig. 4 **a** low-magnification and **b** high-magnification FESEM image of the iron sample prepared in the water system with 20 g of alkaline; **c** low-magnification and **d** high-magnification FESEM image of the iron sample prepared in the ethanol system with 5 g of alkaline

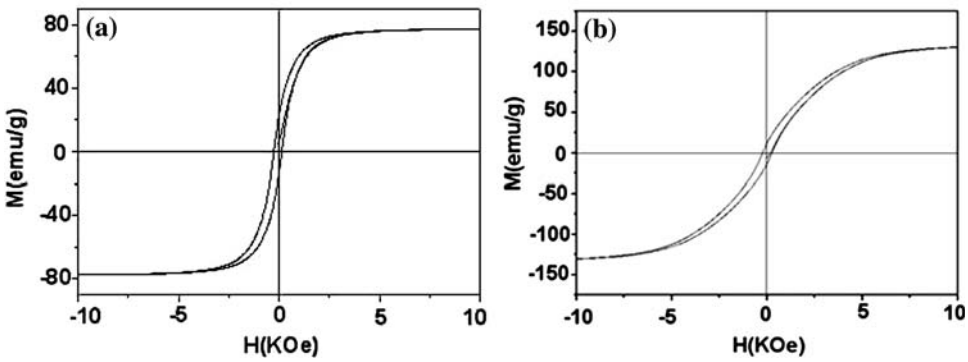

Fig. 5 M-H (magnetization-hysteresis) loops of as-prepared samples measured at room temperature: **a** Fe_3O_4 octahedrons, **b** Fe tubes prepared in the water system

shown in Fig. 5a. The hysteresis loop of the products shows ferromagnetic behavior with saturation magnetization (M_s), remanent magnetization (M_r), and coercivity (H_c) values of about 81, 22 emu/g and 190 Oe, respectively. The saturation magnetization (M_s) value is different from those reported for Fe_3O_4 nanowires (68.7 emu/g) [30] and nanoparticles (85.8 emu/g) [31]. This may be due to the low shape anisotropy and the multiple domains of Fe_3O_4 octahedrons which facilitate magnetization in the directions along their easy magnetic axes. Many factors such as size, structure, surface disorder, morphologies, etc. may influence the magnetic properties of materials. Anisotropy, including crystal anisotropy and shape anisotropy, caused the lower saturation magnetization observed in this work. This plays an important role in reducing the saturation magnetization because most materials contain some type of anisotropy. The H_c and the M_s values are opposite to those expected from the Stoner–Wohlfarth theory: $H_c = 2\ K/(\mu_0\ M_s)$, where K is the magnetocrystalline anisotropy constant and μ_0 is the vacuum permeability [32]. Therefore, the higher H_c leads to a lower M_s for the samples with cubic magnetocrystalline anisotropy. Enhanced anisotropy induces a large magnetic coercivity where the magnetic spins are preferentially aligned along the long axis and their reversal to the opposite direction requires higher energies than for lower shape anisotropy [33]. The order of shape anisotropy was found to be nanowires > octahedrons > nanoparticles. As the shape of anisotropy increases, the H_c increases. When the H_c increases the M_s decreases based on the above considerations.

We also measured the magnetization of the iron samples that were obtained in water. Figure 5b gives their magnetization hysteresis (M-H) loops. The coercivity was 197 Oe which is lower than the reported values for Fe nanorods (900 Oe) [34]. The lower coercivity obtained in this work may be caused by lower anisotropy, which plays a vital role in determining the coercivity of magnetic crystals.

Conclusions

In summary, we prepared novel Fe_3O_4 octahedrons and Fe tubes in different concentrations of alkaline solution by reducing hematite with hydrazine hydrate. Using a high amount of alkaline (20 g), pure iron was produced. By comparison with the reaction in water, the reaction in ethanol required less sodium hydroxide and smaller particles were obtained.

Acknowledgements This work was supported by a Grant-in-aid for Scientific Research from the Japan Society for the Promotion of Science (JSPS), the CREST program of the Japan Science and Technology Agency (JST), the National Natural Science Foundation of China (No. 50873042), and the Scientific Research Program of the HuaiHai Institute of Technology (KQ08023, Z08018). We are grateful to the young and middle-aged academic leaders of the "Blue and Green Blue Project" of the universities and colleges in Jiangsu Province. We are also grateful to the University of Science & Technology of China for assistance in XRD and SEM measurements.

References

1. Kroll E, Winnik FM, Ziolo RF (1996) Chem Mater 8:1594
2. Ni Y, Ge X, Zhang Z, Ye Q (2002) Chem Mater 14:1048
3. Puntes VF, Krishnan KM, Alivisatos AP (2001) Science 291:2115
4. Sheikh AD, Mathe VL (2008) J Mater Sci 43:2018. doi:10.1007/s10853-007-2302-6
5. Suslick KS, Fang M, Hyeon T (1996) J Am Chem Soc 118:11960
6. Park SJ, Kim S, Lee S, Khim ZG, Char K, Hyeon T (2000) J Am Chem Soc 122:8581
7. Chio CJ, Tolochko O, Kim BK (2002) Mater Lett 56:289
8. Cui ZL, Dong LF, Hao CC (2000) Mater Sci Eng A 286:205
9. Sun YP, Rollins HW, Gufuru R (1999) Chem Mater 11:7
10. Nikel DE, Cin JL, Harriso SR, Nikle JA (1996) J Magn Magn Mater 155:67
11. Xu J, Zhang W, Yang Z, Yang S (2008) Inorg Chem 47:699
12. Vayssieres L, Rabenberg L, Manthiram A (2002) Nano Lett 12:1393
13. Chen M, Tang B, Nikles DE (1998) IEEE Trans Magn 34:1141
14. Su XB, Zheng HG, Yang ZP, Zhu YC, Pan AL (2003) J Mater Sci 38:4581. doi:10.1023/A:1027350005911
15. Zhang DE, Ni XM, Zheng HG, Li Y, Zhang XJ, Yang ZP (2005) Mater Lett 59:2011
16. Maillard M, Giorgio S, Pileni MP (2002) Adv Mater 14:1084
17. Ni XM, Zhao QB, Zhang DE, Zhang XJ, Zheng HG (2007) J Phys Chem C 111:601
18. Zhu Y, Zheng H, Yang Q, Pan A, Yang Z (2004) J Cryst Growth 260:427
19. Ban I, Drofenik M, Makovec D (2008) J Magn Magn Mater 307:250
20. Gates B, Yin Y, Xia Y (2000) J Am Chem Soc 122:12582
21. Zhang DE, Ni XM, Zheng HH (2005) J Colloid Interface Sci 292:410
22. Chen L, Yang WJ, Yang CZ (1997) J Mater Sci 32:3571. doi:10.1023/A:1018613926326
23. Zheng H, Liang J, Zeng J, Qian Y (2001) Mater Res Bull 36:947
24. Zheng H, Zeng J, Liang J (1999) Acta Metall Sinica 35:837
25. Wang ZL (2000) J Phys Chem B 104:1153
26. Cheng Y, Zheng YH, Wang YS, Bao F, Qin Y (2005) J Solid State Chem 178:2394
27. Liu Z, Li S, Yang Y, Hu Z, Peng S, Liang J, Qian Y (2003) New J Chem 27:1748
28. Cao XB, Gu L, Zhuge LJ, Qian WH, Zhao C, Lan XM, Sheng WJ, Yao D (2007) Colloids Surf A Physicochem Eng Aspects 297:183
29. Emin S, Sogoshi N, Nakabayashi S, Villeneuve M, Dushkin C (2009) J Photochem Photobiol A: Chem 207:173
30. Wang J, Chen QW, Zeng C, Hou BY (2004) Adv Mater 16:137
31. Wang J, Sun JJ, Sun Q, Chen QW (2003) Mater Res Bull 38:1113
32. Zhao LJ, Zhang HJ, Xing Y, Song SY, Yu SY et al (2008) J Solid State Chem 181:245
33. Seo WS, Jo HH, Lee K, Kim B, Oh SJ, Park T (2004) Angew Chem Int Ed 43:1115
34. Vayssieres L, Rabenberg L, Manthiram A (2002) Nano Lett 2:1393